LA-7107-MS
Informal Report

c.4

UC-48
Issued: February 1978

Development of a Proton Radiographic System for Diagnosis and Localization of Soft-Tissue Abnormalities

Final Report

Kenneth M. Hanson

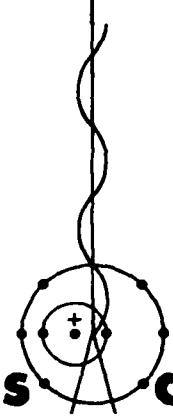

los alamos
scientific laboratory
of the University of California
LOS ALAMOS, NEW MEXICO 87545

An Affirmative Action/Equal Opportunity Employer

UNITED STATES
DEPARTMENT OF ENERGY
CONTRACT W-7405-ENG. 36

Printed in the United States of America. Available from
National Technical Information Service
U.S. Department of Commerce
5285 Port Royal Road
Springfield, VA 22161

Microfiche	$ 3.00	126-150	7.25	251-275	10.75	376-400	13.00	501-525	15.25
001-025	4.00	151-175	8.00	276-300	11.00	401-425	13.25	526-550	15.50
026-050	4.50	176-200	9.00	301-325	11.75	426-450	14.00	551-575	16.25
051-075	5.25	201-225	9.25	326-350	12.00	451-475	14.50	576-600	16.50
076-100	6.00	226-250	9.50	351-375	12.50	476-500	15.00	601-up	--1
101-125	6.50								

1. Add $2.50 for each additional 100-page increment from 601 pages up.

DEVELOPMENT OF A PROTON RADIOGRAPHIC SYSTEM FOR DIAGNOSIS AND LOCALIZATION OF SOFT-TISSUE ABNORMALITIES - FINAL REPORT

by

Kenneth M. Hanson

ABSTRACT

The results of a project to develop a proton computed tomographic (CT) scanning system are reviewed. A high-quality proton CT reconstruction is presented which verifies the substantial dose advantage protons possess over x rays in obtaining CT reconstructions of equivalent density resolution. Furthermore, the unusual aspects of CT reconstruction noise are discussed. Modifications to the Molière theory of multiple Coulomb scattering are described.

I. INTRODUCTION

This document represents the final report on a two-year project funded under the Los Alamos Scientific Laboratory New Research Initiatives Program. The purpose of the project was to develop a practical proton computed tomographic (CT) system at LAMPF for diagnosing and localizing soft-tissue abnormalities. We will discuss dose calculations for proton and X-ray CT scanners which predict a substantial dose advantage for protons over X rays. A subsequent experimental implementation of a proton CT scanner at LAMPF produced CT reconstructions with density resolution comparable to state-of-the-art commercial X-ray scanners at reduced dose. Furthermore, we will discuss the peculiar characteristics of the noise in CT reconstructions which were elucidated in the course of this project as well as modifications to the Molière theory of multiple Coulomb scattering.

II. RECONSTRUCTION ALGORITHMS AND CT NOISE

Several reconstruction algorithms have been implemented on the CDC7600 computer under the LTSS and CROS operating systems. Of the reconstruction algorithms investigated, our version of the well-known filtered backprojection algorithm has proven to be the best for reconstruction from a large number (> 100) of equally spaced views covering a full 180° field of view. We have incorporated Fourier interpolation between projection samples in the backprojection process avoiding the more usual linear interpolation which is time consuming. Another algorithm developed at LASL was that of Fourier interpolation in which the 2-D Fourier transform of the image is obtained directly from the Fourier transforms of the projections. This algorithm proved to produce severe artifacts in the presence of large-density anomalies, making it unsuitable for use.

The general-purpose SNARK program from SUNY (Buffalo) has been implemented on the CDC7600. Included in this program are several versions of the algebraic reconstruction technique (ART) which obtain the reconstruction by iteration. The ART reconstruction algorithms are well suited to situations in which there are a limited number of projections or a limited field of view. It was hoped that the ART algorithms would allow us to improve the spatial resolution attainable with a proton CT scanner. However our experience with the ART routines has indicated that the spatial resolution achieved by them is worse than that obtained with the filtered backprojection algorithm even with perfect projection data. Furthermore, the ART routines were found to be divergent in the presence of noise as the number of iterations increased. Thus, these algorithms were

dropped in favor of filtered backprojection for the purpose of reconstruction of the proton CT data.

The FR-80 and VIDS display systems at the Central Computing Facility have been used to provide gray scale photographs of the reconstructions. Such pictures represent a vast improvement over the earlier isometric plots in picking out details in the images.

An interesting aspect concerning the noise found in CT reconstruction was uncovered by Riederer, Pelc, and Chesler.[1] They found that the process of reconstruction suppresses the low-frequency components of the noise present in the projection data. This implies a long-range negative correlation in the CT noise, provided the projection noise is uncorrelated (white). The effect of this type of noise on the detection capability of the human observer was investigated by the author.[2] It was found that the human eye requires a higher signal-to-noise ratio (SNR) to detect circular objects in the presence of CT noise than in the presence of white noise. Spatial smoothing of the CT images was found to improve the detection of large circles. These preliminary results, if borne out by subsequent investigation, would indicate the existence of a rather interesting feature of the human observer and may well have consequences for CT diagnostic techniques. The noise present in reconstructions from an EMI 5005 scanner was shown[3] to conform with the properties described in reference 2. Recent interest in the application of decision theory to radiographical images[4] invites extension to CT images. Signal detection theory may well provide a basis for optimization of reconstruction algorithms with respect to an "optimum receiver."[5]

III. DOSE CALCULATIONS

In the CT method, the two-dimensional density distribution of a specimen is reconstructed from integrated density ($\int \rho dx$) distributions taken through that section at various angles. The proton CT technique consists of obtaining the integrated density distributions,or projections, by measuring the energy lost by protons which traverse the specimen. The uncertainty in the integrated density is determined by the statistical fluctuations which occur in the energy loss process, commonly called straggling. If the energy lost by the proton is experimentally determined by measuring the residual range of the exiting proton in some specified material, the uncertainty in the integrated density is given by the range straggling. Thus, a single 190-MeV proton, which has a range of 23.6 g/cm^2 in water, can provide integrated density to an accuracy of 0.28 g/cm^2.[6]

In order to explore the usefulness of protons in reducing the dose required to obtain a given reconstruction quality, we have computed the dose needed to produce a reconstruction similar to that obtained by the updated EMI head scanner.[7] It was assumed that a 1.3-cm-thick slice within a specimen is to be examined with picture elements of dimension 1.5 mm x 1.5 mm. The density resolution desired is 0.4% per picture element.

Use of the Shepp and Logan reconstruction algorithm[8] was assumed in the noise calculation. It was also assumed that the projection measurements are taken from a full 360° range of angles. The proton dose was determined from the ionization energy loss. A correction was made for the fraction of incident protons which undergo nuclear interaction rendering them unusable in the energy loss measurement. The X-ray dose was calculated on the basis of the energy absorption coefficient,[9] the backscatter factor and the depth-dose relation.[10] A monoenergetic X-ray beam was assumed. Figures 1 and 2 show the dependence of the required proton and X-ray dose, respectively, upon the particle energy for 10-cm, 20-cm and 30-cm examination diameters. Table 1 summarizes the doses at the optimum particle energies. It is apparent that protons could provide the same density information as monochromatic X rays with a reduction of the dose by a factor of 3.9 for a 20-cm-diameter specimen and a factor of 8.2 for a 30-cm specimen.

IV. MULTIPLE COULOMB SCATTERING AND SPATIAL RESOLUTION

The intrinsic spatial resolution attainable in proton radiography is limited by the multiple Coulomb scattering that protons undergo as they pass through the specimen. The theory of multiple scattering effects in low-Z materials (of which animal tissue is composed) had not been correctly developed. Although the Molière theory[11] is straightforward, its application had become confused in recent years by the introduction of an incorrect center-of-mass

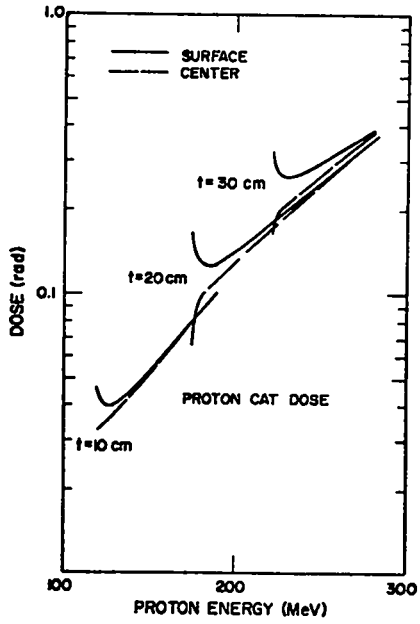

Fig. 1 Relative proton dose required to achieve reconstructions of constant density resolution in fixed pixel sizes.

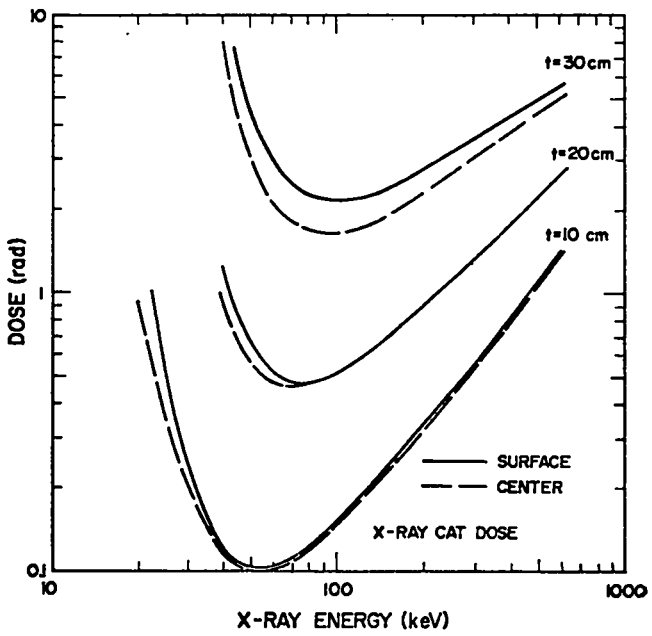

Fig. 2 Same as Figure 1 except for monoenergetic X rays.

TABLE 1

Comparison of Proton and X-Ray Doses Required to Obtain a 0.4% Density Resolution in 1.5 x 1.5 mm^2 Picture Elements for a 13 mm Thick Section of Water-Like Material

PATH LENGTH, P	PROTONS		X RAYS		PROTON DOSE ADVANTAGE
	ENERGY	SURFACE DOSE	ENERGY	SURFACE DOSE	
(g/cm^2)	(MeV)	(rad)	(keV)	(rad)	
10	130	0.010	55	0.026	2.5
20	190	0.032	80	0.12	3.9
30	230	0.065	100	0.53	8.2

transformation to explain discrepancies between the theory and experimental results obtained with 600 MeV protons for several low Z-elements.[12] Considerable attention was paid to this problem because of its importance to proton radiography and pion therapy as well as to several other LAMPF experiments. It was found that the major discrepancies observed with 600-MeV protons were resolved by inclusion of the inelastic scattering of the projectile by the atomic electrons. This was calculated for the Molière theory in 1953 by Fano.[13] Recent atomic form factors[14] and incoherent scattering functions were used to obtain screening parameters for the Molière theory which represent an improvement over Molière's calculations based on the Thomas-Fermi model. A direct relation between the multiple Coulomb scattering theory parameters and the definition of the radiation length[15] was discovered which led to the proper form for the screening correction. It was also found that the above-mentioned atomic form factors yielded radiation lengths which differ from a recent tabulation by Tsai[15] by more than 1% for many elements. The above results will be described in more detail in a publication in preparation.

An experimental test of the modified Molière theory was performed on the EPICS channel at LAMPF in collaboration with W. J. Braithwaite, C. L. Morris, A. W. Obst, E. Smith, and H. A. Thiessen. Data were taken with incident pions, muons, and electrons at a single beam momentum of 151 MeV/c. The targets used included lithium, beryllium, carbon, aluminum, copper, and lead. Figure 3 shows

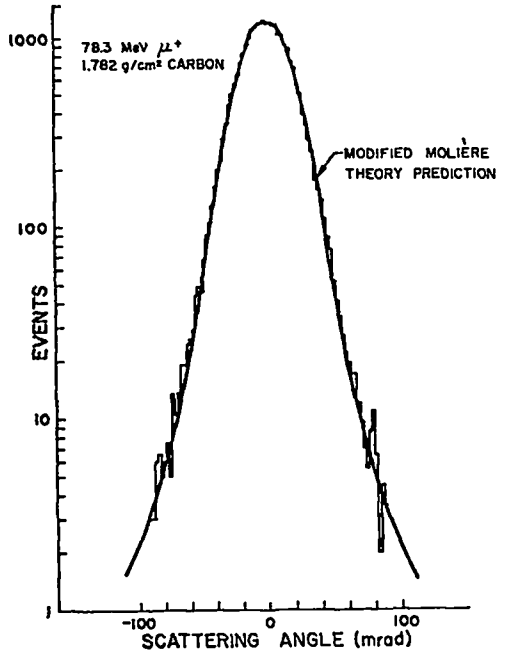

Fig. 3. Comparison between the measured projected angle distribution and that predicted by the modified Molière theory of multiple Coulomb scattering.

preliminary results obtained for μ^+ multiple scattering in carbon. It is seen that there is excellent agreement with the prediction of the modified Molière theory. The data clearly show the transition from a simple Gaussian distribution to that of plural scattering for angles larger than 50 mrad. Over 50,000 events were accumulated for each particle-target combination. It is expected that the analysis of these data will result in measurements of the width of the multiple scattering distributions which are accurate to about 1%.

The Molière theory incorporating the improvements discussed above has been used to determine the spatial spreading of a pencil beam of protons as it passes through tissue. At any depth the central and major portion of the displacement distribution predicted by the Molière theory may be approximated by a Gaussian distribution. The correction to the usual Rossi formula[16] for multiple scattering in water is shown in Figure 4 as a function of the thickness of water. Table II gives equivalent Gaussian widths for the incident proton energies that would be used to examine 20- and 30-cm-thick specimens. These widths represent transverse spatial resolution at the specified depth if the position of the protons

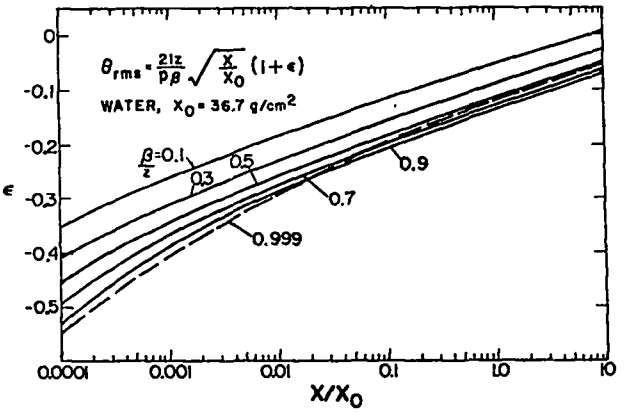

Fig. 4. Correction to Rossi multiple Coulomb scattering formula for effective rms polar angle for water as a function of thickness in radiation lengths (X_o).

TABLE II

Root Mean Square Transverse Displacement of Protons in ICRU Muscle[17] of Unit Density

PROTON ENERGY (MeV)	DEPTH (cm)	RMS RESOLUTION (mm)
190	10	1.2
	20	3.8
230	15	1.9
	30	5.9

were measured only at the entrance to the specimen.

A comparison of the resolutions given in Table II with the rms resolution of present commercial scanners, approximately 1 mm, points to a need to improve the spatial resolution obtainable with protons. One method for obtaining such an improvement is to measure the position of the protons as they exit from the specimen. Another possible approach would be to use heavier charged particles such as alpha particles.[18]

V. EXPERIMENTAL IMPLEMENTATION

An experiment was performed on the P^3 West channel at LAMPF to demonstrate the feasibility of obtaining high-quality CT scans with protons. The approach taken in this experiment was to produce a CT reconstruction with the best density resolution possible with "conventional" detectors and electronics within a reasonable data acquisition period.

The experimental layout is shown schematically in Figure 5. A specially developed tune of the P^3

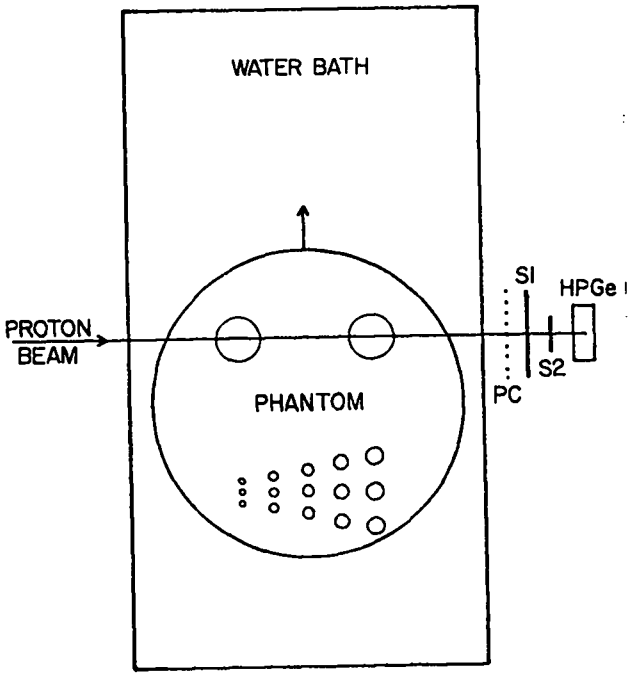

Fig. 5. Schematic layout of proton tomography experiment.

channel provided protons in a momentum bite of 0.2% with a 1.6-mm-wide by 3-mm-high beam spot. The energy lost by each proton was determined from the measurement of the residual proton energy with a hyperpure germanium (HPGe) detector. The HPGe detector was chosen for this experiment on the basis of its excellent gain stability. The HPGe detector had a diameter of 3.3 cm and a thickness of 1.25 cm. The event trigger was obtained from the two scintillation counters, S1 and S2. S2, with an active diameter of 2 cm, restricted the events to the central region in the HPGe detector. A delay line readout proportional chamber PC, was used to measure the transverse deflection of each proton at the exit of the water bath. During the measurements the phantom was moved across the beam line under the computer control. At the end of each traverse, the phantom was rotated by computer command before a new traverse was begun. The use of buffered CAMAC analog-to-digital converters allowed us to acquire data at an average rate of 740 events per sec with 50% deadtime. Further experimental details are presented in reference 19.

It was demonstrated during the course of data taking that the experimental method had sufficient stability to produce high quality tomograms. Specifically, the systematic uncertainty in measurements taken over 10-minute periods was found to be approximately 0.003 g/cm^2 for a 23-g/cm^2-thick piece of polyethylene. Data were also taken for two different types of proton detector: (a) a total energy plastic scintillation counter and (b) a range telescope composed of ten 2.7-mm-thick plastic scintillators. These data will be analyzed to determine the suitability of these types of detectors to a more practical (faster) proton scanner.

A complete set of scan data was taken for both a 20-cm-and a 30-cm-diameter phantom. Sixty-two and a half million events were obtained for the 30-cm phantom in a total running time of 45 hours. The average dose, calculated for a 1-cm-thick slice in a series of scans was 0.6 rad. This dose is based on the number of incident protons needed to produce 62.5 million good events in the experimental geometry used. In Figure 6 the reconstruction of the 30-cm-diameter phantom obtained with the proton data is compared with one obtained with an EMI 5005 X-ray scanner operated in the fast (20-sec) scan mode. The average dose for the EMI scanner is about 2.2 rad. The reconstruction from the proton data made use of the measured proton exit position in order to improve spatial resolution.

In the reconstructions the bottom set of circles provides a means of comparing the low-contrast resolution of these scans. These circles represent a contrast of 1.8% with respect to the background material. It can be seen that the low-contrast resolution of the proton scan is somewhat better in the proton scan than in the X-ray scanner at a dose which is nearly 4 times less. This dose advantage is in rough agreement with the dose calculations when one takes into account that in the present experiment half the protons reaching S1 were not used because they fell outside S2.

Another interesting feature of the comparison between the proton and X-ray scans is that the X-ray scan is decidedly darker in the center than at the edge of the phantom. This variation in reconstructed density is due to the well-known beam hardening artifact which arises from the use of a polychromatic X-ray beam. Protons have the advantage that they are not subject to this type of artifact.

The spatial resolving power of the EMI 5005

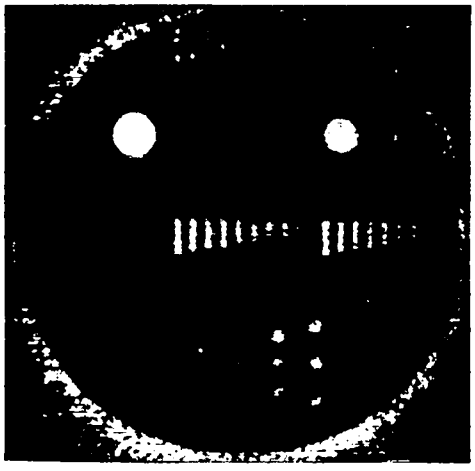

6a

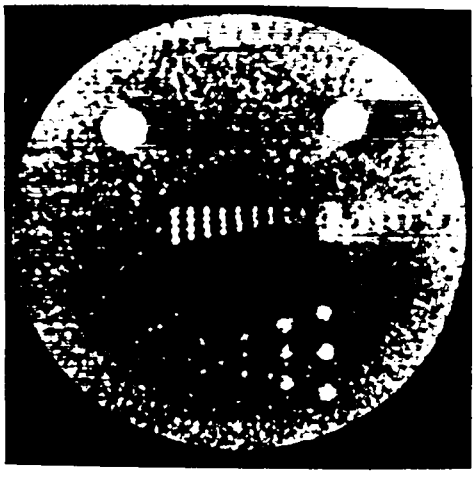

6b

Figs. 6a and 6b. CT reconstruction of the 30-cm phantom obtained with a) protons at a equivalent average dose of 0.6 rads in a 1-cm thick slice and b) EMI 5005 X-ray scanner at 2.2 rads.

measured with the high-contrast (~ 15%) resolution portion of the 30-cm phantom is 1.5 mm. This is somewhat better than that achieved with protons, 2.25 mm. However, it is not clear that this improved spatial resoltuion is advantageous in the presence of a finite noise level, at least for the detection of low-contrast lesions.[2]

VI. FUTURE POSSIBILITIES

Although the proton scan displayed in Fig. 6a took 45 hours to perform, it appears eminently feasible to build a proton scanner that could acquire events at a rate in excess of 1 MHz. Such a scanner would use a scintillation counter range telescope and fast logic to determine proton position and residual range. The data acquisition could be accomplished through the use of special purpose buffered CAMAC modules and a fast CAMAC crate controller.[20] At a 1-MHz data rate, the scan shown in Fig. 6a could be done in 1 minute. At LAMPF, with a duty cycle of 6%, the scan would take about 20 minutes.

The decision to pursue proton CT scanners must be based, in part, on the image contrast of abnormal relative to normal tissue as determined by protons. This proton contrast should be compared to the corresponding X-ray contrast to determine overall effective dose advantage of protons relative to X rays. Dr. Steward, a radiologist at the University of Chicago, has seen several cases in which standard proton radiography with film has revealed abnormal tissue in autopsy specimens which could not be visualized with standard X-ray radiography.[21] This is encouraging but his data must be analyzed in detail to determine whether the advantage of protons in these cases is principally due to the higher overall contrast in the proton images (thus overcoming the detection threshold of the eye) or is due to increased stopping power contrast between the two types of tissue.

VII. SUMMARY

Of the several reconstruction algorithms investigated, the filtered backprojection algorithm was chosen to be most appropriate for a large number of equally spaced views. The peculiar characteristics of the type of noise present in CT reconstructions were explored. The effect of this type of noise on detectability by human observers was studied. Improvements were made in the Molière theory of multiple Coulomb scattering. The calculated dose advantage of protons over X rays in computed tomography was substantiated experimentally. Proton CT scans were performed which resulted in reconstructions of quality comparable to those produced by present-day commercial X-ray scanners. It is concluded that the construction of a 20-minute proton scanner at LAMPF would be feasible.

ACKNOWLEDGMENTS

The author would like to acknowledge Douglas Boyd for providing the EMI scan of the phantom used in the proton CT experiment.

REFERENCES

1. S.J. Riederer, N.J. Pelc, and D.A. Chesler, "Statistical Aspects of Computed X-Ray Tomography," presented at 4th Int. Conf. on Medical Physics, Ottawa, Canada, 1976 and submitted to Phys. Med. Bio.

2. K.M. Hanson, "Detectability in the Presence of Computed Tomographic Reconstruction Noise,"in Proc. SPIE Vol. 127, Proc. Conf. on Appl. of Op. Instr. in Medicine VI, Boston, Massachusetts, 1977, pp. 304-312.

3. K.M. Hanson and D.P. Boyd, "The Characteristics of Computed Tomographic Reconstruction Noise and Their Effect on Detectability," to be published in the IEEE Trans. on Nucl. Sci., Proc. Nucl. Sci. Symp., San Francisco, California, 1977.

4. R.F. Wagner, "Decision Theory and the Detail Signal-to-Noise Ratio of Otto Schade," to be published in Photogr. Sci. and Eng.

5. A.D. Wahlen, Detection of Signals in Noise (Academic Press, New York, 1971).

6. R.M. Sternheimer, Phys. Rev. 117, 485-488 (1960).

7. D.P. Boyd, M.T. Korobkin, and A. Moss, SPIE 96, Op. Instr. in Med. V, 303-312 (1976).

8. L.A. Shepp and B.F. Logan, IEEE Trans. Nucl. Sci. NS-21, 21-43 (1974).

9. R.D. Evans, Radiation Dosimetry, 2nd Ed., F.H. Attix and W.C. Roesch, Eds. (Academic Press, New York, 1968).

10. H.E. Johns and J.R. Cunningham, The Physics of Radiography, 3rd Ed. (Charles C. Thomas, Springfield, 1969).

11. V.G. Molière, Z. Naturforschg. 3a, 78-95 (1948).

12. E.V. Hungerford et al., Nucl. Phys. A197, 515-528 (1972).

13. U. Fano, Phys. Rev. 93, 117-120 (1954).

14. J.H. Hubbell et al., J. Phys. Chem. Ref. Data 4, 471-538 (1975).

15. Y.S. Tsai, Rev. Mod. Phys. 46, 815-851 (1974).

16. B. Rossi, High Energy Particles (Prentice-Hall, Englewood Cliffs, 1952).

17. Physical Aspects of Irradiation, Recommendations of the International Commission on Radiological Units and Measurements, Natl. Bur. Std. (USA) Handbook 85 (1964).

18. T.F. Budinger et al., "Transverse Section Imaging with Heavy Charged Particles: Theory and Application," in Proc. Image Processing for 2D and 3D Reconstruction from Projections (Stanford, California, 1975).

19. K.M. Hanson et al., "The Application of Protons to Computed Tomography," to be published in IEEE Trans. on Nucl. Sci., Proc. Nucl. Sci. Symp., San Francisco, California, 1977.

20. D.R. Machen et al.,"Multi-microprocessor Auxiliary Crate Controller for Front End Data Processing in CAMAC," to be published in IEEE Trans. on Nucl. Sci., Proc. Nucl. Sci. Symp., San Francisco, California, 1977.

21. V.W. Steward, Recent Results in Cancer Research, Vol. 51, 88-96 (Springer-Verlag, Berlin, 1975).